New formulation of the discrete element method

Jerzy Rojek, Aleksander Zubelewicz, Nikhil Madan, and Szymon Nosewicz

Citation: AIP Conference Proceedings **1922**, 030009 (2018);
View online: https://doi.org/10.1063/1.5019043
View Table of Contents: http://aip.scitation.org/toc/apc/1922/1
Published by the American Institute of Physics

New Formulation of the Discrete Element Method

Jerzy Rojek[1,a)], Aleksander Zubelewicz[2], Nikhil Madan[1] and Szymon Nosewicz[1]

[1]*Institute of Fundamental Technological Research,*
Polish Academy of Sciences, Pawinskiego 5B, 02-106 Warsaw, Poland
[2]*Faculty of Civil Engineering, The University of New Mexico, USA*

[a)]Corresponding author: jrojek@ippt.pan.pl

Abstract. A new original formulation of the discrete element method based on the soft contact approach is presented in this work. The standard DEM has been enhanced by the introduction of the additional (global) deformation mode caused by the stresses in the particles induced by the contact forces. Uniform stresses and strains are assumed for each particle. The stresses are calculated from the contact forces. The strains are obtained using an inverse constitutive relationship. The strains allow us to obtain deformed particle shapes. The deformed shapes (ellipses) are taken into account in contact detection and evaluation of the contact forces. A simple example of a uniaxial compression of a rectangular specimen, discretized with equal sized particles is simulated to verify the DDEM algorithm. The numerical example shows that a particle deformation changes the particle interaction and the distribution of forces in the discrete element assembly. A quantitative study of micro-macro elastic properties proves the enhanced capabilities of the DDEM as compared to standard DEM

INTRODUCTION

The discrete element method (DEM) is a powerful tool for predicting the behaviour of various particulate and non-particulate materials such as soils, powders, rocks, concrete, or ceramics [1, 2, 3, 4]. In the DEM, a material is represented by a large assembly of particles (discrete elements) interacting with one another by contact. Two different approaches to contact treatment in the DEM can be identified, the so-called soft-contact approach [5] and the hard-contact concept [6]. In the soft-contact DEM formulation, the particles are treated as pseudo-rigid bodies with deformation concentrated at the contact points. A small overlap of the particles is allowed and it is considered as equivalent to the particle deformation at the contact point. In this approach, the duration of contact is assumed to be much larger than the time step and contact force evolution is determined. The soft-contact approach allows to adopt a suitable contact model and thus resulting in an intended macroscopic behaviour.

The material properties in DEM cannot be prescribed directly, rather they emerge from the collective response of the aggregate and depend on the choice of the interparticle contact model as well as the discrete element assembly characteristics [7]. An appropriate representation of the macroscopic properties in the discrete element method is still a challenge and it is sometimes difficult or impossible to obtain a required deformation behaviour [8]. Some limitations of the discrete element method are due to the assumption of the rigidity of discrete elements.Their deformability would allow to enrich modelling capabilities of the DEM. The simplest way to introduce deformability in the discrete element method is to discretize discrete elements with finite elements [9]. This approach is computationally very expensive and it cannot be used for a large number of particles.

An alternative approach is by adding deformation modes to a rigid motion of discrete elements [10, 11]. Until now this concept has been applied to the discrete elements in the form of polygonal prisms (in 2D) or polyhedra (in 3D). This work presents an original formulation of the discrete element method based on the soft contact approach with deformable circular discs. The developed numerical algorithm has been implemented in the discrete element program developed by the author of this paper. Numerical results will be presented in order to verify the developed theory.

Computer Methods in Mechanics (CMM2017)
AIP Conf. Proc. 1922, 030009-1–030009-6; https://doi.org/10.1063/1.5019043
Published by AIP Publishing. 978-0-7354-1614-7/$30.00

CLASSICAL FORMULATION OF THE DISCRETE ELEMENT METHOD

Based on key assumptions of Cundall and Strack [5], a 2D formulation of the discrete element method employing cylindrical particles (cylindrical discs) is considered in this work. Fundamental formulations of the discrete element method have been presented in a number of publications [12, 13, 14]. However, for the sake of completeness formulation of the contact model is presented here shortly.

Considering a pair of interacting particles, say i and j, with the radii R_i and R_j, shown in Fig. 1. Vectors $\mathbf{x_i}$ and $\mathbf{x_j}$ denotes the positions of the particle centroids. Velocities of particle centroids are described by translational components $\mathbf{v_i}$ and $\mathbf{v_j}$, and the rotational components $\boldsymbol{\omega}_i$ and $\boldsymbol{\omega}_j$

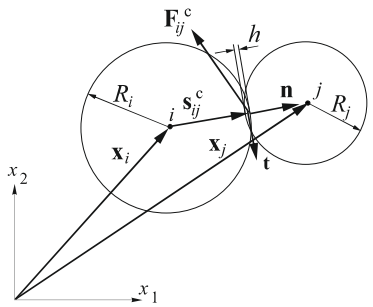

FIGURE 1. Definition of the inter-particle interaction

The particle interaction is described by the bonded particle contact model. In the formulation of this contact model the contact force $\mathbf{F}^{c}$ is decomposed into the normal and tangential components, $\mathbf{F}_{n}$ and $\mathbf{F}_{t}$, respectively:

$$\mathbf{F}^{c} = \mathbf{F}_{n} + \mathbf{F}_{t} = F_{n}\mathbf{n} + \mathbf{F}_{t}\,, \tag{1}$$

where $\mathbf{n}$ is the unit normal vector at the contact point (Fig. 1). Different models can be employed to evaluate the normal and tangential contact forces[15, 16].

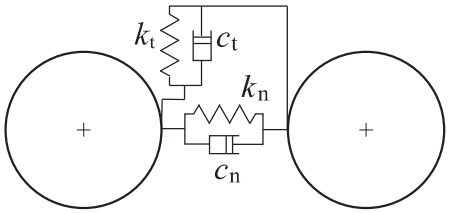

FIGURE 2. Rheological scheme of the bonded particle interaction model.

In this work, the normal and tangential particle interactions are modelled by linear springs connected in parallel with dashpots (Fig. 2) providing an additional mechanism to dissipate contact oscillations. Thus, the normal and tangential contact forces are decomposed into the elastic, F_{ne} and $\mathbf{F}_{te}$, and damping parts, F_{nd} and $\mathbf{F}_{td}$, respectively:

$$F_{n} = F_{ne} + F_{nd} \tag{2}$$

$$\mathbf{F}_{t} = \mathbf{F}_{te} + \mathbf{F}_{td} \tag{3}$$

The elastic contact force components are evaluated assuming linear constitutive relationships. The elastic normal force is given by

$$F_{ne} = k_{n}h\,, \tag{4}$$

where k_n is the interface stiffness in the normal direction, and h is the change of the distance between the particles with respect to the distance when the cohesive bond has been established

$$h = \|\mathbf{x}_j - \mathbf{x}_i\| - R_i - R_j \tag{5}$$

The tangential elastic force is given by the relationship

$$\mathbf{F}_{\mathrm{t}} = k_{\mathrm{t}}\,\mathbf{u}_{\mathrm{t}}\,, \tag{6}$$

where k_{t} is the interface stiffness in the tangential direction, $\mathbf{u}_{\mathrm{t}}$ – the relative displacement at the contact point in the tangential direction.

The contact damping forces in the normal and tangential directions are given by

$$F_{\mathrm{nd}} = c_{\mathrm{n}} v_{\mathrm{rn}} \tag{7}$$

$$\mathbf{F}_{\mathrm{td}} = c_{\mathrm{t}} \mathbf{v}_{\mathrm{rt}} \tag{8}$$

respectively, where c_{n} and c_{t} are the damping coefficients. The damping coefficients, c_{n} and c_{t}, can be related to the critical damping in the normal and tangential direction, $c_{\mathrm{n}}^{\mathrm{cr}}$ and $c_{\mathrm{t}}^{\mathrm{cr}}$, by means of certain scaling factors, ξ_{n} and ξ_{t}:

$$c_{\mathrm{n}} = \xi_{\mathrm{n}} c_{\mathrm{n}}^{\mathrm{cr}} \tag{9}$$

$$c_{\mathrm{t}} = \xi_{\mathrm{t}} c_{\mathrm{t}}^{\mathrm{cr}} \tag{10}$$

For the system of two rigid bodies with masses m_i and m_j, connected with a spring of the stiffness k, the critical damping c^{cr} is given by, cf. [17]:

$$c^{\mathrm{cr}} = 2\sqrt{\frac{m_i m_j k}{m_i + m_j}} \tag{11}$$

By taking $k = k_{\mathrm{n}}$ or k_{t} in Eq. (11) the critical damping $c_{\mathrm{n}}^{\mathrm{cr}}$ and $c_{\mathrm{t}}^{\mathrm{cr}}$ is obtained.

FORMULATION OF THE DEFORMABLE DISCRETE ELEMENT METHOD

We shall consider a discrete element model consisting of cohesionless or cohesive cylindrical particles subjected to a prescribed external loading. The idea of the DDEM is shown in Fig. 3.

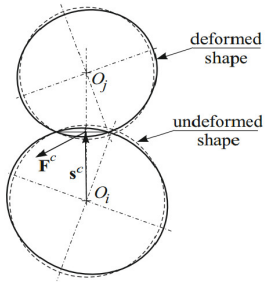

FIGURE 3. The idea of deformable discrete element method.

In addition to standard kinematics of the discrete element method, in our new formulation particles are assumed to be uniformly deformed under the internal particle stress induced by the contact forces. A uniform stress is assumed in the particle. The internal particle stress $\overline{\sigma}_p$ is obtained as the average stress derived from the contact forces using the following formula [18]:

$$\bar{\boldsymbol{\sigma}}_p = \frac{1}{V_p} \sum_{c=1}^{n_{pc}} \frac{1}{2} \left(\mathbf{s}^c \otimes \mathbf{F}^c + \mathbf{F}^c \otimes \mathbf{s}^c \right), \tag{12}$$

where V_p is the particle volume, n_{pc} number of elements being in contact with the particle, $\mathbf{s}^c$ vector, connecting the particle center with the contact point, $\mathbf{F}^c$ contact force, and the symbol $\otimes$ denotes the outer (tensor) product. In case of a constrained particle, except for contact forces we have also reaction forces.

Particle strains are calculated using an inverse constitutive relationship

$$\boldsymbol{\epsilon}_p = \mathbf{D} : \boldsymbol{\sigma}_p \tag{13}$$

where $\mathbf{D}$ is the elastic compliance tensor for the plane strain.

The circular configuration under a uniform strain is deformed into an elliptical one with its principal axes aligned to the principal strain directions. The normal contact force is determined as a linear function of the overlap of such ellipses. This overlap is considered as equivalent to local deformation of the particles. Similarly, as in the standard DEM the local damping is included in the normal interaction. The tangential contact force is evaluated similarly as in the standard DEM.

NUMERICAL EXAMPLE

A uniaxial compression of a rectangular specimen discretized with bonded discs as it is shown in Fig. 4 has been simulated using the standard and new DEM formulation. A bonded particle contact model has been used. The sample is a regular assembly of 180 particles each of radius $r = 1$ mm, arranged in 20 rows and 9 columns. Total sample height H is 40 mm and width A is 18 mm. A particle density $\rho = 2000$ kg/m^3 and normal contact stiffness $k_n = 7 \cdot 10^{10}$ N/m has been assumed. A uniform linear load (0 to 10 kN in 0.1 ms) is applied on each column from top and bottom. The maximum value total force F has achieved is 90 kN.

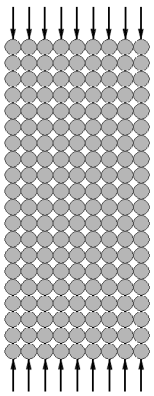

FIGURE 4. Uniaxial compression of a rectangular specimen – DEM model

Figure 5 shows the results obtained with the standard DEM formulation in the form of the contours of displacements along the y and x axes. It can be seen that all the elements have zero x displacements. This means that the macroscopic effective Poisson's ratio is zero in this model under the loading along the y axis. Figure 6 shows the results obtained with the new DEM formulation. One can notice non-zero displacements in the x direction which implies a non-zero Poisson's ratio. This shows that the new formulation allows us to capture the Poisson's effect even in such a simple configuration of discs where standard DEM fails. This confirms new capabilities of the proposed formulation with respect to the standard DEM.

A quantitative investigation has been conducted in order to study the influence of particle (microscopic) elastic parameters on global (macroscopic) elastic parameters. Simulations are performed by keeping a constant normal contact stiffness $k_n = 7 \cdot 10^{10}$ N/m. The particle Young's modulus E_p varies in range $2{\cdot}10^{10}$ N/m^2 – $8{\cdot}10^{10}$ N/m^2 (k_n/E_p in the range $0.350 - 0.0875$). A constant value of particle Poisson's ratio $\nu_p = 0.35$ is assumed. Figure 7 presents the effect of the particle parameters – contact stiffness k_n and particle Young's modulus E_p on global parameters – macroscopic Young's modulus E_{DDEM} and macroscopic Poisson's ratio ν_{DDEM}.

From Fig.7 we can deduce that the global (macroscopic) stiffness in the DDEM is lower than that obtained in standard DEM. Moreover, lower particle Young's modulus E_p (or equivalently, the higher k_n/E_p ratio) results in lower global stiffness in DDEM. It also shows that the stiffness in the DEM – E_{DEM} coincides with the stiffness of the DDEM model – E_{DDEM} for $k_n/E_p \to 0$ (or equivalently $E_p \to \infty$), which corresponds to the basic assumption of the standard DEM that the particles are rigid with deformation localized at contact areas. Similar behaviour can also be observed

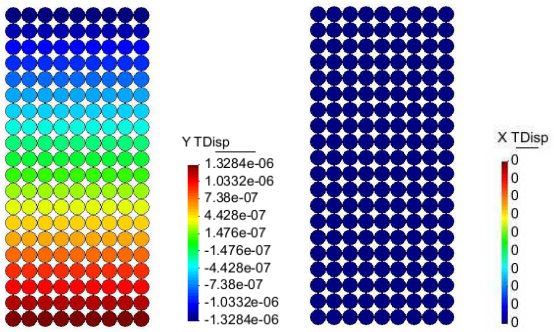

FIGURE 5. Simulation results obtained with the standard DEM formulation – contours of displacements along, the y-axis (*left*), the x-axis (*right*) at $t = 0.0001$ s. Particle Young's modulus $E_p = 2 \cdot 10^{10}$ N/m^2.

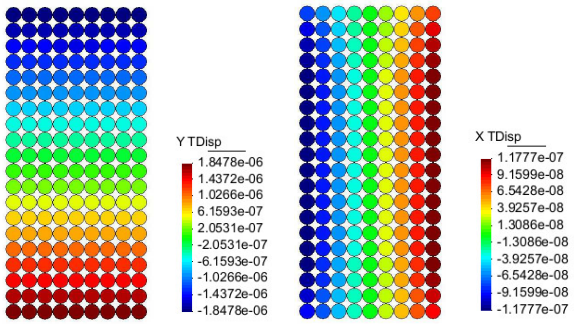

FIGURE 6. Simulation results obtained with the deformable DEM formulation – contours of displacements along, the y-axis (*left*), the x-axis (*right*) at $t = 0.0001$ s. Particle Young's modulus $E_p = 2 \cdot 10^{10}$ N/m^2.

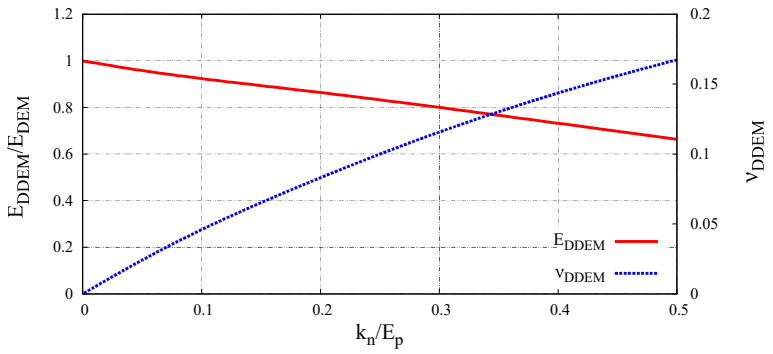

FIGURE 7. Influence of particle elastic parameters on the global elastic parameters – Ratio of global Young's modulus in the deformable and standard DEM and global Poisson's ratio as a function of ratio k_n/E_p. Particle Poisson's ratio $\nu_p = 0.35$ is used.

for Poisson's ratio in Fig. 7, where as $k_n/E_p \to 0$ (or equivalently $E_p \to \infty$) the Poisson's ratio of DDEM model ν_{DDEM} coincides with Poisson's ratio of standard DEM model ν_{DEM} which is equal to 0 cf. Fig. 5. Results presented in Fig. 7 can provide us a basis for the quantitative study of a more realistic, irregular particle assembly.

CONCLUSIONS

Numerical example has shown that by taking deformability of particles into account, the modelling capabilities of the DEM has been enhanced. The non-local contact interactions which appear due to global deformation (shape change) of the discrete particles can introduce Poisson's effect even in simple assemblies where standard DEM fails. The new formulation introduces a greater flexibility in terms of controlling the elastic behaviour of a particulate system and allows for better representation of deformation modes of particles.

A quantitative investigation has been conducted to evaluate the influence of micro elastic parameters on macro elastic parameters. The DDEM model is able to reproduce the behaviour of standard DEM model as the limit case. The quantitative relationships can be used in studying more realistic particle configurations. The proposed formulation is equally valid for cohesionless DEM models and can be easily extended to 3D problems.

ACKNOWLEDGMENTS

This work has been financed from the funds of Polish National Science Centre (NCN) awarded by the decision number DEC-2015/19/B/ST8/03983.

REFERENCES

1 S. Hentz, L. Daudeville, and F. Donze, ASCE J. Eng. Mech. **130**, 709–719 (2004).
2 J.Rojek, E. Onate, C. Labra, and H. Kargl, International Journal of Rock Mechanics and Mining Sciences **48**, 996–1010 (2011).
3 R. Senapati and J. Zhang, "Identifying fracture origin in ceramics by combination of nondestructive testing and discrete element analysis," in *Progress in Quantitative Nondestructive Evaluation*, AIP Conference Proceedings 1, edited by D. O. Thompson and D. E. Chimenti (American Institute of Physics, Melville, NY, 2010), pp. 1445–1451.
4 L. Widulinski, J. Kozicki, and J. Tejchman, Archives of Hydro-Engineering and Environmental Mechanics **56**, 149–171 (2009).
5 P. Cundall and O. Strack, Geotechnique **29**, 47–65 (1979).
6 D. Hong and J. McLennan, Phys. A: Stat. Mech. Applicat. **187**, 159–171 (1992).
7 J. Rojek, C. Labra, O. Su, and E. Onate, Int. J. Solids and Structures **49**, 1497 – 1517 (2012).
8 C. O'Sullivan, J. D. Bray, and L. Cui, "Experimental validation of particle-based discrete element methods," in *GeoCongress 2006*, edited by D. F. Don J. DeGroot, Jason T. DeJong and L. G. Baise (American Society of Civil Engineers, Reston,VA, 2006), pp. 1–18.
9 A. Munjiza, *The Combined Finite – Discrete Element Method* (Wiley, West Sussex, England, 2004).
10 P. Cundall, T. Maini, J. Marti, P. Beresford, N. Last, and M. Asgian, Computer modeling of jointed rock masses, U.S. Army Engineers Waterways Experiment Station, Technical Report N-78-4 (1978).
11 J. Williams and G. Mustoe, Computers and Geotechnics **4**, 1–19 (1987).
12 P. Cundall, International Journal of Rock Mechanics and Mining Sciences and Geomechanics Abstracts **25**, 107 – 116 (1988).
13 R. Hart, P. Cundall, and J. Lemos, International Journal of Rock Mechanics and Mining Sciences & Geomechanics Abstracts **25**, 117 – 125 (1988).
14 J. Rojek, C. Labra, O. Su, and E. Onate, International Journal of Solids and Structures **49**, 1497 – 1517 (2012).
15 H. Kruggel-Emden, E. Simsek, S. Rickelt, S. Wirtz, and V. Scherer, Powder Technology **171**, 157–173 (2007).
16 H. Kruggel-Emdena, S. Wirtz, and V. Scherer, Chemical Engineering Science **63**, 1523–1541 (2008).
17 L. M. Taylor and D. S. Preece, Engineering Computations **2**, 243–252 (1992).
18 S. Luding, Int. J. Solids and Structures **187**, 159–171 (2004).